AD-A124 229 THE EFFECTS OF TRANSVERSE STRESS ON MAGNETIZATION(U) 1/1
NAVAL ACADEMY ANNAPOLIS MD J M RICHARDSON 1982
USNA-TSPR-119

UNCLASSIFIED F/G 11/6 NL

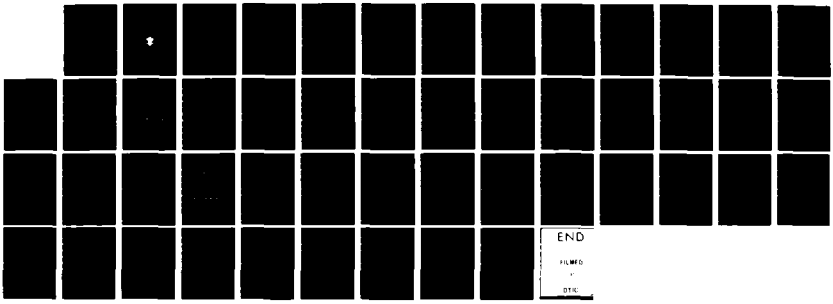

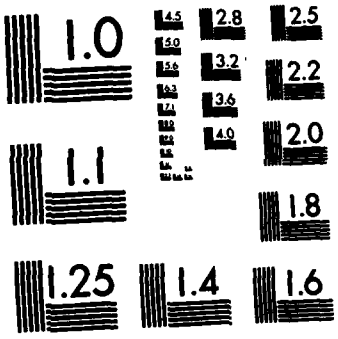

MICROCOPY RESOLUTION TEST CHART
NATIONAL BUREAU OF STANDARDS-1963-A

(9)

AD A124229

A TRIDENT SCHOLAR PROJECT REPORT

NO. 119

THE EFFECTS OF TRANSVERSE STRESS ON MAGNETIZATION

UNITED STATES NAVAL ACADEMY
ANNAPOLIS, MARYLAND
1982

DTIC FILE COPY

This document has been approved for public release and sale; its distribution is unlimited.

DTIC ELECTE FEB 9 1983 A

83 02 09 003

U.S.N.A. - Trident Scholar project report; no. 119 (1982)

"The Effects of Transverse Stress on Magnetization"

A Trident Scholar Project Report

by

Midshipman

John M. Richardson, 1982

U. S. Naval Academy

Annapolis, Maryland

Carl S. Schneider

Professor Carl S. Schneider- Physics

Accepted for Trident Scholar Committee

Chairman

29 July 1982

Date

ABSTRACT

The effects of transverse stress on the magnetization of 3NiCr steel were derived and observed in terms of three separate contributions. First, the previously determined stress-effective field was examined for transverse stress, and agreed with the results obtained in past experiments. A reversal of the effects of tension and compression was predicted and observed.

Second, the stress-sensitive reluctance was found to behave linearly with tensile strain. The experimentally observed slope of 1.55±.05 correlated with the derived value of 1.60±.06. A lower limit to the reluctance was seen in compression.

The third effect was the fractional populations of stress-active domain walls. This is a newly postulated effect which accounts for large-scale changes in domain structure due to the application of external stress. The fractional populations of field-enhancing domain walls was observed to be equal to that od filed-reducing walls. Furthermore, the total population of stress-active walls was found to be a function of applied stress.

Accession For
NTIS GRA&I ☑
DTIC TAB ☐
Unannounced ☐
Justification
By
Distribution/
Availability Codes
Avail and/or
Dist Special
A

DTIC COPY INSPECTED 2

ACKNOWLEDGEMENTS

It is impossible to complete a project of this magnitude alone. I have received support and assistance from many people throughout the year, and I am deeply grateful. I would like to specifically thank the David Taylor Naval Ship Research and Development Center, the Mechanical Engineering Department, the Engineering Technical Support Division, and the Department of Physics at the U.S. Naval Academy for their cooperation in this endeavor.

A special thanks and deep respect is reserved for Professor Carl S. Schneider, without whom this project could never have been completed. Independent research can be rewarding, but reward comes after hard work, disappointment, and failure along the way. Professor Schneider offered his expertise, support, and the occasional firm hand needed to keep this project moving.

TABLE OF CONTENTS

SUBJECT	PAGE
Abstract	1
Acknowledgements	2
Table of Contents	3
Section I - Theory	4
Section II - Experimental Apparatus	19
Section III - Data and Analysis	24
References	39
Appendices:	
Appendix A- Derivation of Important Equations	40
Appendix B- Schneider's Restatement of Kondorsky's Law	42
Appendix C- Analysis of 3NiCr Steel	43
Appendix D- Index of Symbols Used	44

SECTION I - THEORY

The magnetization of ferromagnetic materials is affected both by the application of an external magnetic field, and by stress applied to the material. Stress effects on magnetization were first examined in the early 1800's by Mateucci, Villari and others. Since those first experimental studies, there have been many contributions to a better understanding of the stress dependence of magnetization. It is the purpose of this study to determine stress effects on the magnetic behaviour of U.S. Navy shipbuilding steels. The sample used in this research was fabricated of 3NiCr steel, which is the material used in the construction of some Navy ships. The sample was subjected to external fields well beyond the coercive field, and stress well beyond the residual stress of the material, in both tension and compression. In all instances, the stress was applied perpendicular (transverse) to the external field.

Magnetization in materials takes place by the alignment of electron spins. The total magnetization is due to the additive effect of these spins. There is an exchange

energy between the electrons in a material such that they tend to align themselves along an easy axis in the crystal lattice. For the 3NiCr sample used, the easy axis is the <100> axis. It is easy to saturate the material along one of these directions, and it is much more difficult to magnetize the material in any other direction. This preferred orientation of magnetization is due to the anisotropy energy of the material. In a single crystal, this energy is extremely significant.

It is clear that all electron spins in a given sample of ferromagnetic material are not aligned parallel to each other. The net magnetization of most materials is close to zero, which would not be the case if the material were saturated in a single direction.

To account for the net zero magnetization, Pierre Weiss introduced the concept of domains: a domain is a small region in the material which is magnetized to saturation in a given direction. There are very many domains that constitute the entire material, each saturated in a different direction, so that the net magnetization over the whole material averages close to zero. This concept has been verified, and domains have been observed directly.

Domains are formed inside a material due to the reduction of magnetostatic energy. By the opposition of two magnetic domains, each saturated in opposite directions, the energy is greatly reduced from the case of a single domain.

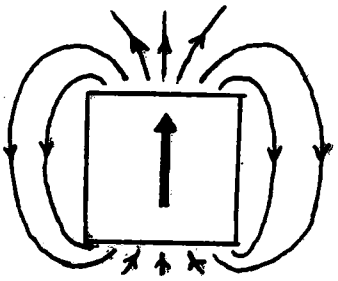

FIGURE 1

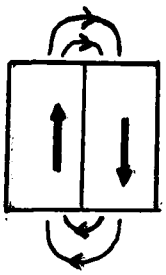

Single Domain
Greater Magnetostatic Energy

Opposed Domains
Reduced Magnetostatic Energy

The continued reduction of magnetostatic energy would drive the material to divide infinitely. The equalizing factor is the fact that it requires energy to form a domain wall between two domains. Domain subdivision stops when the total energy is a minimum.

Taking domains into consideration, there are two ways in which the net magnetization in a material may be changed. The first method is through the movement of domain walls. By increasing the volume of domains saturated in a particular direction(while simultaneously decreasing the volume of those saturated in other directions), a net magnetization can result. This mechanism is referred to as domain wall translation. The second way that magnetization can take place is through rotation. This occurs when the direction of magnetization within a domain is altered from its easy axis. These two processes are illustrated in Figure 2.

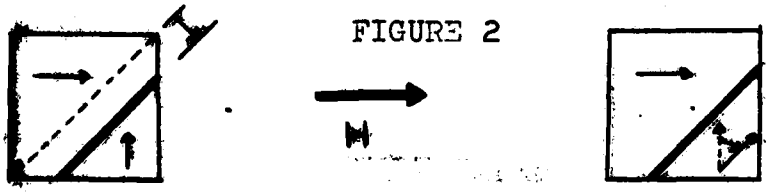

FIGURE 2

Wall Translation

Rotation

When a magnetizing force is applied to the material, both of these effects occur simultaneously. However for low fields, the wall translation effect dominates, whereas the rotation effect dominates for higher fields, well above the coercive field.

Each of the domains in a material has with it an associated energy. In a more complete analysis, the energy within a domain is:

$$1)\ E = \frac{k}{4}\sin^2(2\theta_{mk}) + \frac{3}{2}\lambda_s\sigma\sin^2(\theta_{m\sigma}) - HM_s\mu_0\cos(\theta_{mH}) + \frac{\mu_0 D M_s^2}{2}\cos(\theta_{mD})$$

In the first term, the anisotropy energy, k is the anisotropy constant for the material, and θ_{mk} is the angle between the easy axis(<100>) and the magnetization. The second term of the equation is the magnetoelastic energy where λ_s is the saturation magnetostriction, σ the applied stress, and $\theta_{m\sigma}$ the angle between the direction of applied stress and the direction of magnetization. The third term is the magnetostatic term. In this term H is the applied field, M_s is the saturation magnetization, $\mu_0 = 4\pi \times 10^{-7}$ N/A^2, and θ_{mH} is the angle between field and magnetization. The fourth term is the demagnetization energy where D is the demagnetization constant for the sample(a factor which depends on the shape of the sample), and θ_{mD} is the angle between the demagnetization and the magnetization.

It is advantageous at this time to consider one of the terms of the domain energy equation. This term is

the anisotropy energy. This energy is associated with the rotation of the magnetization within a domain of the material. If the energy is minimized for the anisotropy energy and the field energy, one finds that the rotation-related field is:

2) $H_k = \frac{k}{2\mu_0 M_s}$

For our material, the anisotropy constant k is 4300 J/m^3. This results in a related field H_k = 40,000 A/m, which is many times the fields applied during the course of the experiments.

Similarly, if one minimizes the energy of the anisotropy and stress, the relation is:

3) $\sigma_k = \frac{k}{3\lambda_s}$

This related stress is of the order $\sigma_k = 5.38 \times 10^8$ J/m^3, which is many times the limits imposed by this experiment. From the large values obtained for the equivalent field and stress as they are related to the anisotropy energy, it is assumed that this energy does not change a significant amount in the course of the experimental process, and the anisotropy energy will be treated as a constant for the purposes of this research.

There is another contribution to the energy that is not expressed in Equation (1). This is an energy due to the internal stresses within the material. Internal stresses arise when the material is heated and cools unevenly, when it is bent or twisted, or when it is machined.

These are small, evenly distributed stresses inside the bulk of the material, independent of any externally applied stress. The internal stresses for our material are characteristically on the order of 6×10^7 N/m^2, which is comparable to the stresses applied to the material during the course of the experiments. This energy is seen to have definite effects when the applied stress is equal to or less than the internal stress.

Now that these two quantities have been examined, the dominant stress effects on magnetism will be treated. R.R. Birss[1] stated that the magnetization of ferromagnetic materials due to stress depended on three effects: 1. Direct pressure on the domain walls; 2. Changes in the opposition to domain wall movement; 3. Large scale changes in domain structure. Each of these effects will now be considered separately.

When stress is placed on a ferromagnetic material, there is a consequent pressure that exerts itself directly on the domain walls, causing them to move. This translation will result in a change in the magnetization of the material. W.F. Brown[2] examined the effects of this direct pressure and suggested that in relation to stress, there were three distinct types of domain walls. In Figure 3, three types of domain structures are illustrated.

FIGURE 3

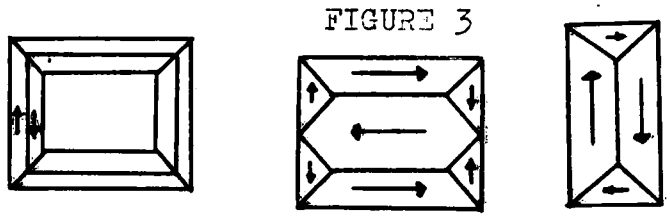

Closure Domain Configurations

From the figure, one can see that the boundaries between adjacent domains are either at a 90° or 180° angle with the domain direction. Brown deduced, from the $\sin^2(\theta_{ms})$ dependence in the magnetoelastic energy term of Equation (1), that the 180° walls were not affected by stress. Furthermore, he stated that the 90° walls are divided into two groups: those that will move to enhance the field with tension (90+), and those that will move to oppose the field in tension (90-). The contributions of these two types of walls are reversed with the application of compression((90-) walls increase the field with compression and (90+) walls decrease the field with compression). The contributions of each of these wall types were plotted by Brown on a magnetization curve for a process whereby the sample is demagnetized, an external field is applied, and tension is applied and removed. C.S. Schneider[3] extended this process to include the application of a compression and release. Schneider's results are shown in figure 4.

In this graph, which shows the magnetization of the sample due to the applied field and stress, the individual contributions of each type of stress-effective wall are shown. First, the sample is magnetized by an external

field up to point (A).

FIGURE 4

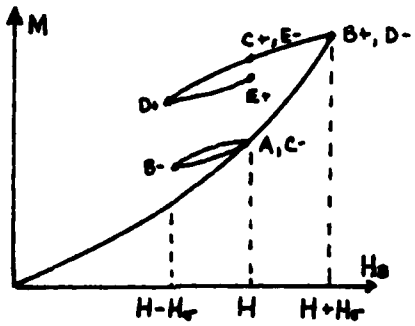

Contribution of Stress-Active Walls
for Tension-Compression Cycle

A tension is applied which gives rise to a stress-effective field H where:*

4) $H_\sigma = \frac{3\lambda_s \sigma}{\mp 2M_s \mu_0}$

During this process, the (90+) walls continue to magnetize the sample up to point B+, where the (90-) walls decrease the magnetization down to point B-. The (90-) walls do not retrace the original path of magnetization, but are subject to a hysteresis. This was described by Kondorsky[4], and restated by Schneider in the form:

5) $\chi'(\Delta H) = \chi\left(\frac{\Delta H}{2}\right)$

where $\chi = dM/dH$, the differential susceptibility of the material. This relation states that if a material is magnetized with a field H, and subject to a decrease in field ΔH(such as that imposed by the movement of (90-) walls), the susceptibility will be that of the half-argument

*Equation (4), and all others are derived from Equation (1) in Appendix A. They are omitted here in the interest of continuity.

of the original field, $\frac{\Delta H}{2}$. This relation is derived in Appendix E. This effect is only applicable to a reversal of field, so the (90+) walls continue to increase the magnetization along the original line. Schneider continued the process to the release of tension(points C+ and C- for (90+) walls and (90-) walls respectively), application of compression (D+, D-), and release of compression (E+, E-). Kondorsky's Law applies upon all effective field reversals.

From Equation (1) the stress and field energy terms are:

$$E = \frac{3\lambda_s\sigma}{2}\sin^2(\theta_{mr}) - HM_s\cos(\theta_{mr})$$

By minimizing this energy, and applying the conditions for transverse stress, one arrives at the relation:

$$6)\quad H_\sigma \text{ (transverse)} = \frac{\pm 3\lambda_s\sigma}{2M_s}$$

Comparison of Equation (4), which was derived for the uniaxial stress-field condition employed by Schneider, and Equation (5), which is the relation derived for transverse stress-field, reveals that they are equivalent except for a sign reversal. The physical significance of this sign change is that the effects of tension and compression are reversed for the two cases. A material subjected to transverse stress will behave in tension the same way the material subjected to uniaxial stress will behave in compression. This reversal arises from the angular dependence of the application of stress and field seen in Equation (1).

Equation (5) is the governing equation for the effect

of direct pressure on domain walls. It is seen to be a linear effect with stress. This direct pressure effect is only one of the three effects that stress has on a material. The next one to be addressed is the variations in opposition to domain wall movement.

There are properties of a material, such as inclusions, impurities, internal stresses, and grain boundaries which serve to hinder the movement of domain walls through the material. They are obstacles against which domain walls may be pinned. The configuration of these obstacles is altered with the application of external stress, which in turn alters their opposition to domain wall movement. As a domain wall moves through an inclusion in the material, it sets up small domain structures as shown in Figure 5.

FIGURE 5

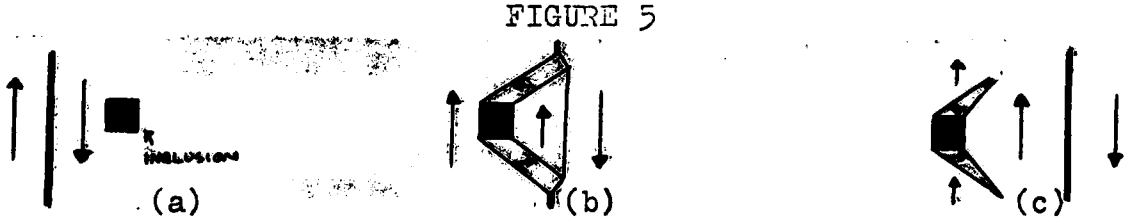

Domain Wall Movement
Through an Inclusion

A stress placed on the sample will cause changes in the configuration of the spikes shown in Figure (5c), and alter the magnetization in the sample. This opposition has been suggested before by two French physicists, Lliboutry[5], and Neël[6].

As a prelude to examining the opposition to wall movement, or reluctance as it is called, the susceptibility will be considered. The susceptibility is the rate at which a

material responds to a magnetizing force. Expressed mathematically this is:

$$\chi = \frac{dM}{dH_{eff}}$$

where χ is the susceptibility, M is the magnetization of the material, and H_{eff} is the effective interior field inside the material. The effective interior field is smaller than the externally applied field:

7) $H_{eff} = H_a - DM$

where H_a is the applied field, D is the demagnetization factor for the sample, and M is the magnetization of the sample. Thus, the interior field is diminished inside the sample by the demagnetizing field which is established inside the sample to oppose the applied field. This demagnetizing field arises from the geometry of the sample and the establishment of magnetic poles at points of discontinuity.

For ferromagnetic materials, there are two contributions to the susceptibility:

8) $\chi_{in} = \chi_{rot} + \chi_{tran}$

where χ_{in} is the total inherent susceptibility, χ_{rot} is that part of the susceptibility due to the rotation mechanism, and χ_{tran} is the component of the susceptibility due to the translation mechanism. The rotational part of the susceptibility(χ_{rot}) is very small in relation to the translational part, due to the large anisotropy energy discussed before. The total inherent susceptibility in our material is dominated by the translational component and most of

the magnetization that occurs is due to domain wall motion.

The reluctance, or opposition to the movement of domain walls is inversely related to the susceptibility, and can be expressed as follows:

$$9)\quad \chi^{-1} = \frac{1}{\chi_{in}} + D + \frac{3\lambda_s}{2\mu_0 M_s^2}(\sigma)$$

where χ^{-1} is the reluctance,

χ_{in} is the total inherent susceptibility, D is the demagnetization factor, and the final term is derived from the magnetoelastic energy of the material(see Appendix A for this derivation). Equation (9) represents a linear equation in stress

$$K = A + B(\sigma)$$

where

$$10)\quad A = \frac{1}{\chi_{in}} + D$$

is a constant involving properties of the material, and

$$11)\quad B = \frac{3\lambda_s}{2\mu_0 M_s^2}$$

is the slope of the line.

Equation (9) is the governing equation for the effect of the changes in the opposition to domain wall translation, the stress-dependent reluctance. Two of the three effects have been examined in detail and have been shown to be simple, linear relations with the application of external stress. The final parameter, the large scale alterations to domain structure, will now be given attention.

The two effects described so far have been analyzed

with the assumption that the general domain structure remains unchanged with the application of stress. In their work involving stress-effective fields, both Schneider and Brown treated the amount of stress sensitive walls to be constant. Furthermore, they assumed that the population of (90+) walls was equal to the population of the (90-) walls. This must by no means be the case. The reorientation of domain walls due to stress will have an effect on the magnetic behavior of the material. This effect was suggested by R.R. Birss as large-scale changes in domain structure.

As stated before, the establishment of domains is due to an energy balance between the magnetostatic energy and the domain wall energy. If a great deal of energy is introduced through the application of stress, the energy balance will be altered and new domain structure will result. This redistribution of domains will give rise to two changes that will affect the magnetization of the material. First, there will be a change due to the change in total domain wall area within the material. Second, as these new domain walls move, they will sweep out different volumes than the original walls did. These two effects, the wall area and the domain volume effects, will be treated together as a single variation due to the change in wall populations. This cumulative effect will be symbolized in this paper by the variable (f). If the total contribution to the energy is normalized such that the

total population, (f_T), is unity, then this total population is divided into the three distinct wall types listed below.

1. (f+) = the fraction of the total population that consists of (90+) walls, and increases the magnetization with tension.

2. (f-) = the fraction of the total population that consists of (90-) walls, and increases the magnetization with compression.

3. (f_o) = the fraction of the total population that consists of (180) walls, and are not affected by stress. The sum of the fractions must add up to the total population, which has been normalized to unity, such that

12) $(f+) + (f-) + (f_o) = (f_T) = 1$

Thus, the population factor, (f), accounts for the large scale domain changes by separating the contributions of (90+), (90-), and (180) walls.

In review, three effects on the variation of magnetization with stress have been examined. They are: the linear stress-effective field arising from direct pressure on domain walls; the stress-sensitive reluctance, which comes from the variation of the opposition to domain wall motion; and the scaling of wall populations due to large alterations in domain structure. These effects have been symbolized by H_σ, χ_σ, and (f) respectively. In a mathematical form, taking these factors into account, the magnetization change in a material can be expressed by the relation:

13) $\Delta M = \int \sum_{i=0} (f_i)\chi_e(H_i)dH_i$

where the summation is made over the contributions of the three different wall types.

Equation (13) describes the change in magnetization, dM, in terms of the three variables discussed. If these three processes were to act simultaneously, it would be very difficult to extract any information from the data taken due to the complexity of the curves. It was the aim of all experiments to subdue or control two of the three parameters in order to study the third alone. In the treatment that follows, it will be seen that quite complex changes can be interpreted as the simultaneous effects of some remarkably simple relationships.

SECTION II-

EXPERIMENTAL APPARATUS

The material used for the experiments was 3NiCr steel, the same steel used in the construction of U.S. Navy ships hulls(an analysis of 3NiCr is given in Appendix C). A hollow cylinder was machined from a solid sample of the material. The dimensions of the cylindrical sample are given in Figure (6). There were two rows of holes drilled at each end of the cylinder. Each row consisted of ten holes, spaced equally around the walls of the cylinder and drilled radially through the walls. The area of the sample between the two outer rows of holes is referred to as the 'active' region, as it was the portion of the sample that was magnetized during the experiments.

Outside the active region, each end was reinforced and threaded to accommodate mounts to the stress-application mechanism. Stress was applied by means of an Instron automatic stress machine. The Instron was capable of applying stress at a controllable rate, and of maintaining the sample in a fixed state of stress

FIGURE 6

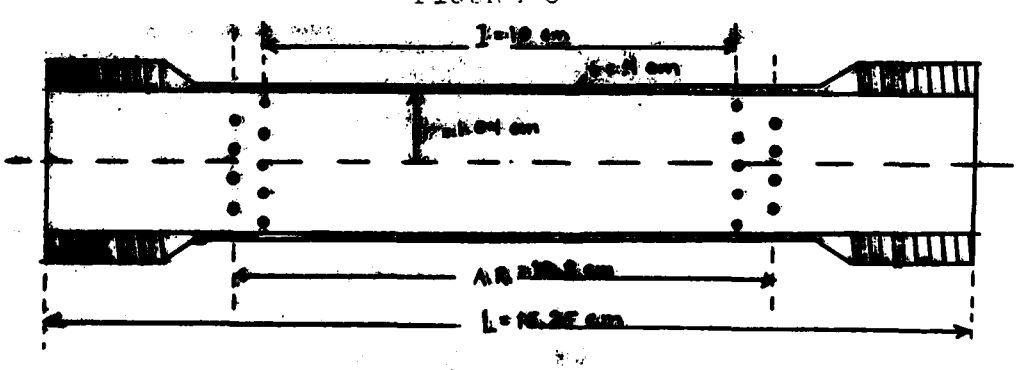

Cylindrical Sample

In order to measure the stress on the sample, a strain gauge bridge was applied to the outer wall of the cylinder. The voltage across the bridge was maintained precisely at a predetermined value which provided a readout where ten microvolts corresponded to one microstrain. The type of strain gauge used was accurate for readings up to 1400 microstrains. The dimensionless quantity of strain is related to stress by the following equation:

$$\text{strain} = \frac{\Delta l}{l} = \frac{\text{stress}}{E}$$

where E= Young's Modulus for 3NiCr steel.

A field was applied azimuthally around the walls of the cylinder by means of a wire coil (H-coil) of 100 turns wound between the two innermost holes on the sample(Figure 7). There were ten turns wrapped through each pair of holes to provide a uniform distribution around the walls of the cylinder. A current, controlled by an amplifier and function generator, was sent through the H-coil which applied a field given in Equation (14):

$$\oint H \cdot dl = nI \qquad \text{(Ampere's Law)}$$

$$H(2\pi r) = nI$$

$$H = \frac{nI}{2\pi r} = \frac{nV_H}{2\pi r R_H} \tag{14}$$

where H is the applied field, n is the number of turns in the H-coil, r is the radius of the cylinder, I is the current in the coil, R_H is the resistance of the H-coil, and V_H is the voltage across the coil. Because of heating effects, the current in the H-coil was limited to 1.4 amperes, which corresponds to a maximum applied field of 2150 A/m. The transverse relation-

ship between stress and field is shown in Figure (7).

FIGURE 7- Stress-Field Relationship

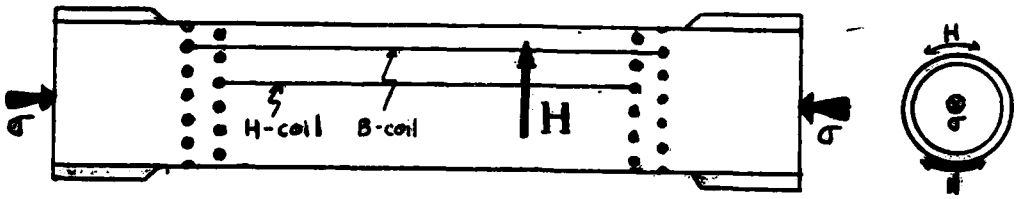

Another coil of 100 turns was wound between the two outer rows of holes. This coil (B-coil) was the pickup coil which sensed the magnetic field induced in the sample. The voltage across the B-coil was related to the magnetism by the following relation:

$$V_B = n\left(\frac{d\phi}{dt}\right) \qquad \text{(Faraday's Law)}$$

where V_B is the voltage across the B-coil, n is the number of turns in the B-coil, and ϕ is the magnetic flux through the coil. The value for $d\phi/dt$ was obtained by use of an integrator with a time constant RC:

$$\frac{d\phi}{dt} = \frac{AB}{RC}$$

where A is the area enclosed by the B-coil, and B is the magnetism in the sample. Substituting this into the above equation,

$$V_B = \frac{nAB}{RC} \qquad \text{or}$$

$$15) \qquad B = \frac{RCV}{nA}$$

The complete experimental apparatus is pictured in Figure (8):

FIGURE 8 - EXPERIMENTAL APPARATUS

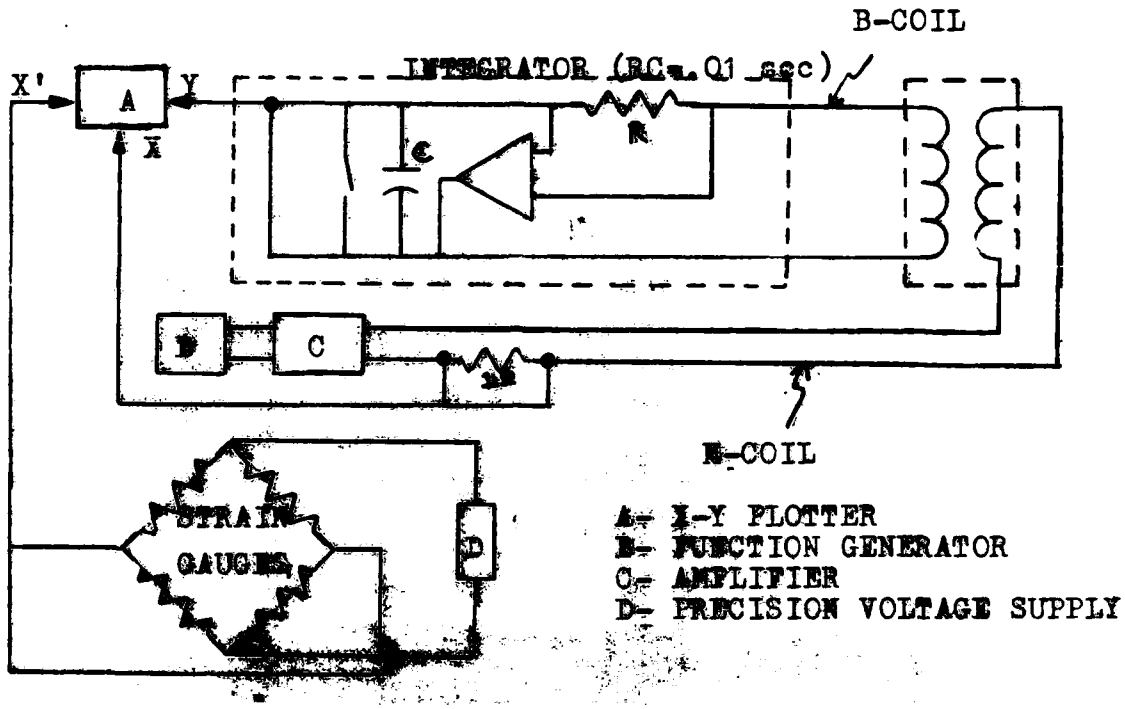

The closed circular geometry around the walls of the cylinder was advantageous in that the demagnetization factor for the sample was very small. The only contributions to the demagnetizing field arose from the establishment of small magnetic poles at the holes through which the H-coil was wound, plus some other higher order effects in the region between the two rows of holes at each end. In addition to the small demagneting field, the closed geometry was a benefit in that any spurious fields from the surrounding environment did not affect the measurements; the only fields that were measured were those controlled by the experimental apparatus.

The apparatus proved to give excellent results except in the region of very small stresses. In this region, there was a stalling effect due to the backlash in the mounting of the sample. There was also a deviation because of the initially unbalanced application of stress to the sample. This imbalance came from machining variations in the construction of threads in the mounts to the sample. These two effects resulted in an uncertainty in the stress readout for small stresses, which was removed for stresses greater than fifty microstrains. This is the region where all the experiments were conducted.

SECTION III-

DATA AND ANALYSIS

Using the apparatus described in Section II, experiments were devised to examine the three stress effects which determine the magnetization in the material. As was mentioned before, the magnetization curves in which all three parameters are acting simultaneously are difficult to interpret without an understanding of how each effect behaves individually. In order to obtain this understanding, experiments were constructed that would suppress the contributions of two of the three effects, so that the third could be closely examined. The results of these experiments are presented here.

A.) Direct Pressure on Domain Walls

As has been explained in Section I, the application of external stresses puts pressure directly on domain walls. This pressure forces the walls to move, giving rise to a change in magnetization. This change in magnetization is due to the stress-effective field, symbolized by the character H.

The stress-effective field for 3NiCr was derived and measured by C.S. Schneider in 1980. A review of his work will serve as the discussion for this effect.

The primary difference between Schneider's experiments and mine is that his work involved uniaxial stress and field, whereas this research investigates transverse stress and field. An examination of the thermodynamics involved in the two cases quickly reveals that for the stress-effective field, there is

only one difference between uniaxial and transverse stress.

Equation (4) gives the stress-effective field to be:

$$H_\sigma = \pm\frac{3\lambda_s\sigma}{2M_s\mu_0}$$

The derivation for the uniaxial case yields the same result, with the exception of a sign reversal. This arises from the angular dependence of the magnetoelastic term in Equation (1). This reversal was observed experimentally, just as predicted.

Schneider conducted an experiment whereby an 3NiCr sample was put in a field H=79 A/m, and sixty-six microstrains in tension and compression was applied. Two symmetric stress cycles, one beginning in tension and the other in compression, were imposed. The ratios of the two halves of the cycles were compared. A graph of this process is shown in Figure (9):

FIGURE 9

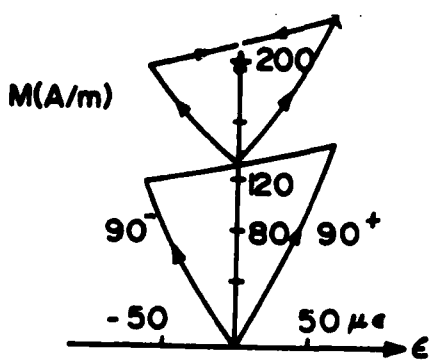

Schneider had determined, from a restatement of Rondorsky's Law in the Rayleigh region, that the ratio between the two half-cycles (r) should be:

$$r = \frac{\Delta M_+}{\Delta M_-} = \frac{(1+\alpha/4)}{(1-\alpha/4)}$$

where $H_\sigma = \alpha H$. The experimental value for the ratio was determined to be r = 1.60 ± .02, which lead to the relation:

$$H = 1.09\ \frac{A/m}{\mu\epsilon}(\epsilon) \qquad (\epsilon = \text{applied strain})$$

in excellent agreement with the derived value in Equation (4) when the appropriate constants for 3NiCr are substituted.

In summary, the **effective field** was found by Schneider to be an effect that is linear with stress. This linear relation was discovered to be the same for transverse stress, with the exception that the effects of tension and compression were reversed. Now that the stress-effective field has been examined, an analysis of the experiments that determined the stress-sensitive reluctance will be given.

B.) Opposition to Domain Wall Movement

The second effect that contributes to stress-induced magnetization is the reluctance, χ^{-1}, and its variation due to stress. The susceptibility, χ, is the rate of change of magnetization with field.

$$\chi = \frac{dM}{dH_{eff}}$$

In order to measure the stress-sensitive susceptibility, the sample was placed in a fixed stressed state. The susceptibility was measured by applying a field (H) to the sample in this state. The stresses were varied and readings were taken for each value of applied stress. Figure (10) displays the results of these measurements.

Curve C is the susceptibility for zero applied stress. The peak occurs at χ =1520, H =700 A/m. As the sample was subjected to compression, the peak susceptibility increased and occurred at a slightly lower applied field. These peaks moved gradually upward with increased compression until a strain of 500 microstrains was reached, where a limit occurred. No

further increase in the peak susceptibility was observed for stresses greater than 500 microstrains in compression. This limit is thought to be due to a finite level of demagnetization, inclusions, and other defects in the material which prevent the susceptibility from becoming any greater.

FIGURE 10 - Stress-Sensitive Susceptibility

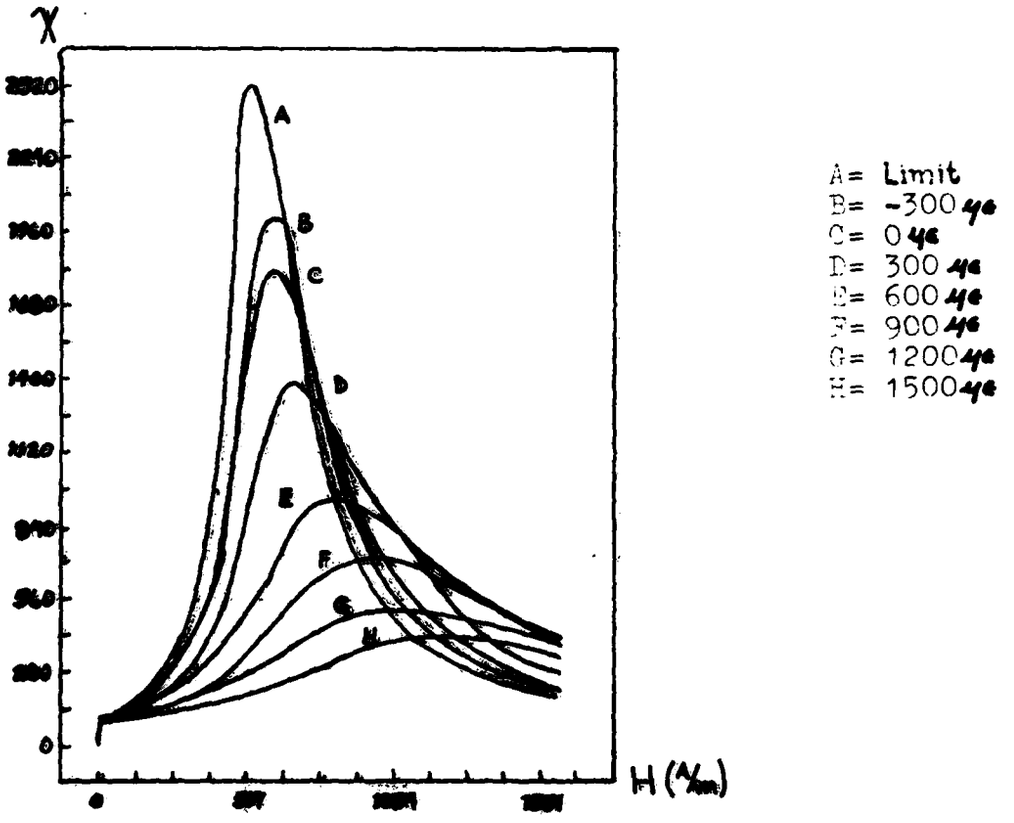

In tension(curves D-H) the maximum susceptibility was gradually decreased, occurring at higher values of applied field. No limiting value was seen in tension and the peaks decreased smoothly.

The peak of each curve corresponding to the maximum susceptibility occurs at the same effective field inside the sample. Although the applied field may vary, the effective field,

given by Equation (7), remains the same and is called the coercive field. Because the effective field at the peaks is constant, it is possible to graph the peak value of susceptibility against the value of the stress corresponding to that peak. This plot is shown in Figure (11):

FIGURE 11

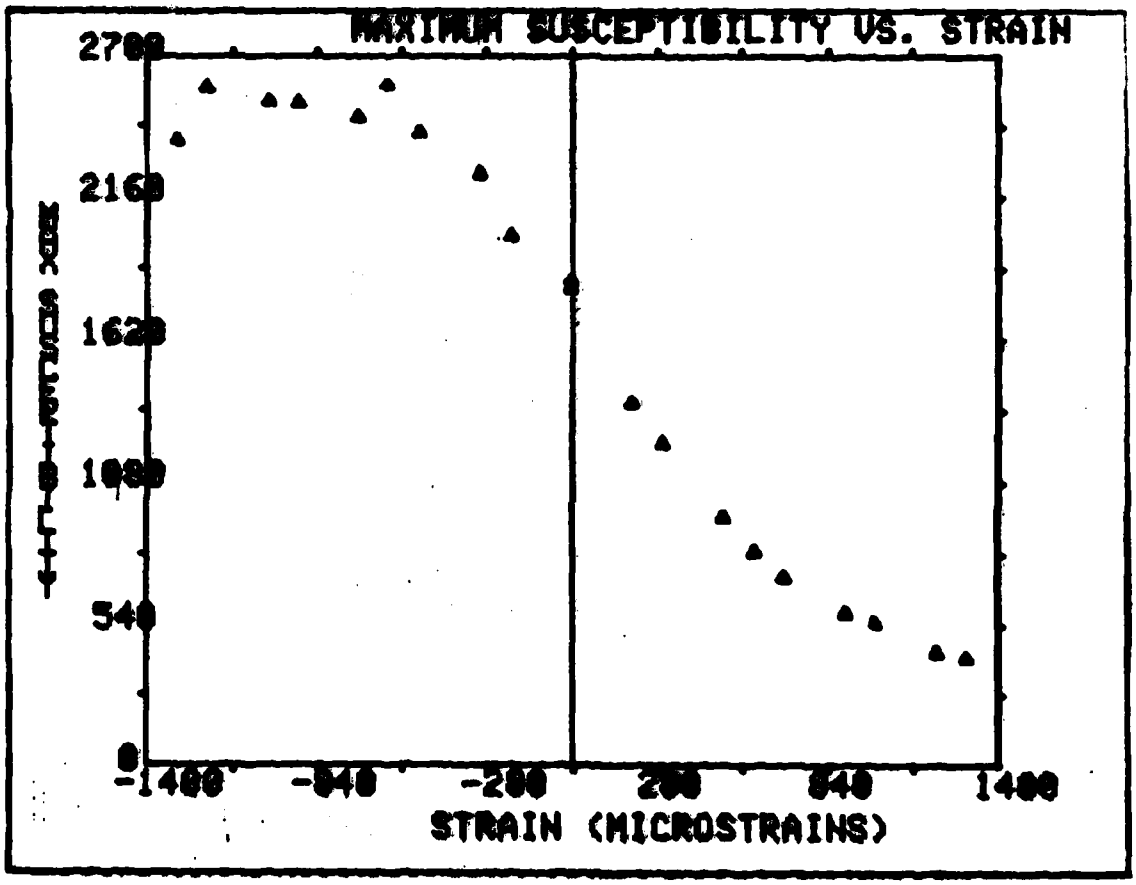

In this graph, one can see the limiting value of susceptibility for stresses less than -500 microstrains, and the smooth decrease through the zero stress point and for applied tension.

As was discussed in Section I, the stress-sensitive susceptibility is related to the reluctance through the inverse

proportionality given in Equation (9). When a plot is made of the reluctance against stress, a linear behavior results, as shown in Figure (12):

FIGURE 12

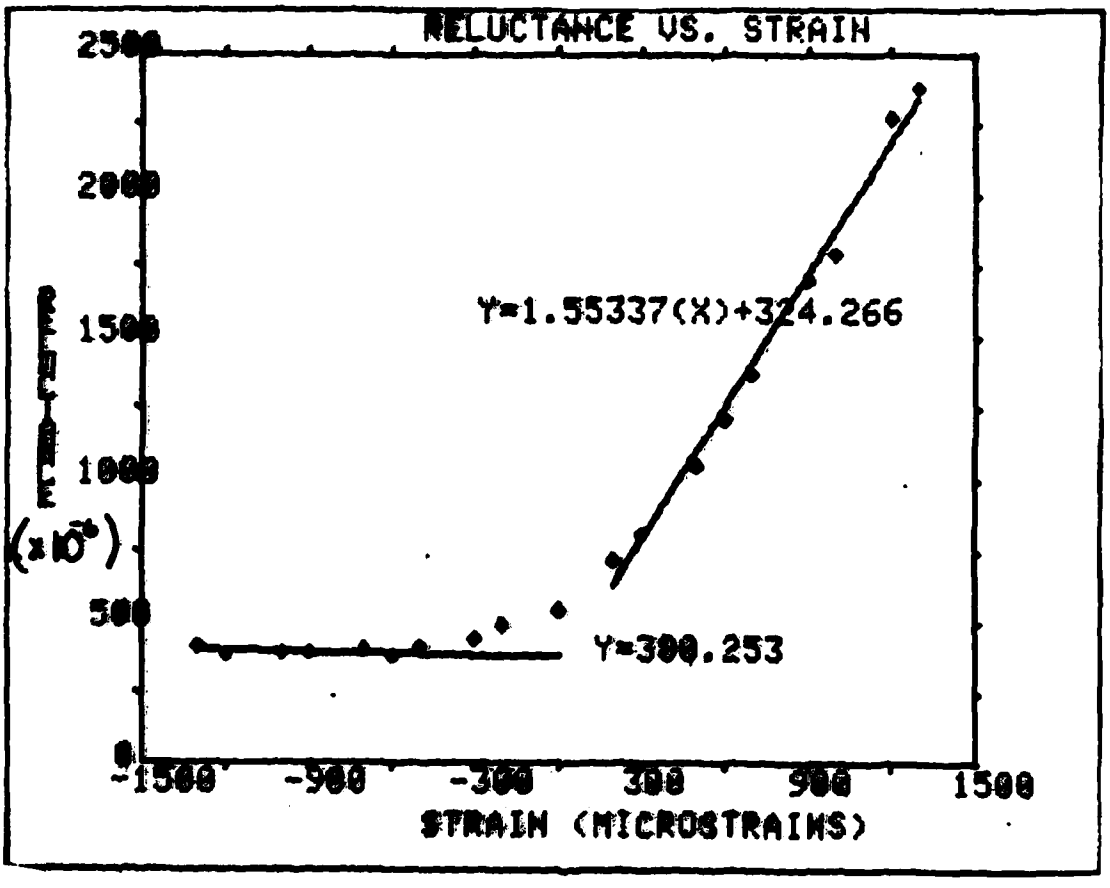

This graph shows a positive slope for tensile stresses and an asymptotic value for compressive stresses. This limiting reluctance is the same effect as the maximum values obtained for the susceptibility in high compression. It is the lower limit of reluctance for this particular material, where there is no longer any contribution due to the stress-sensitive reluctance.

According to Equation (9), the slope for the linear portion of the graph, when the constants for 3NiCr are sub-

stituted is 1.61 ± .06. A least-squares fit of the data results in a slope of 1.55 ± .05, in good agreement.

There is a deviation of the data from the linear behavior expected as the plot crosses through the origin. This curvature, which occurs in the region ±300 microstrains, is due to a contribution of internal stresses to the stress- sensitive reluctance. As was mentioned in Section I, when the externally-applied stress is of the same magnitude as the internal stresses, the internal stresses have an impact on the stress-sensitivity of the material. At values of large externally applied stress in tension or compression, the applied stress dominates the internal stresses, and the linear behavior is observed. In the region between ±300 microstrains, the internal stresses have the effect whereby the reluctance is seen to curve smoothly through the zero stress point.

The agreement between the derived value and the observed slope suggests that the stress-sensitive reluctance is given by Equation (9). The theoretical equation for χ^{-1} does not predict the limit seen in the data. This asymptotic behavior is interpreted as being independent of the stress-sensitive contribution. This is reasonable when one considers the effect of inclusions and other obstacles on the free translation of domain walls through the material. The conclusion is that the linear behavior is seen in tension only, and that any variances under compression are due solely to the contribution of internal stresses.

The final experiments were designed to examine the population fractions (f) of the various types of stress-active

walls.

C. Large Scale Alterations in Domain Structure

It was necessary to measure the populations of stress-active walls both in a compressive state and in a tensile state. In order to do this, a field (H) was applied, and the sample was subjected to 178 microstrains in tension. From this value of stress, small tension and compression cycles of fifty-seven microstrains were applied to the sample. For the tension cycles, the increase in magnetization is due to the (90+) walls. For the compressive cycles, the magnetization is due to the (90-) walls. After recording the magnetization due to the tension cycles and the compression cycles, an equivalent field (h) was applied to the sample. The magnitude of this field was determined by Equation (4). All domain walls in the sample are field sensitive, so they will all contribute to the magnetization of the sample when the field (h) is applied. If one takes the ratio of the magnetization due to the tension cycle to that induced by the field, the ratio is equivalent to (f+). Similarly, if one takes the ratio of the magnetization induced by the compression cycles, the ratio will be (f-). The tension and compression cycling was done for average strains of 178 microstrains in tension and compression, and for initially applied fields H = 258, 310, 362, and 414 A/m. This experimental process is schematically illustrated in Figure (13).

FIGURE 13

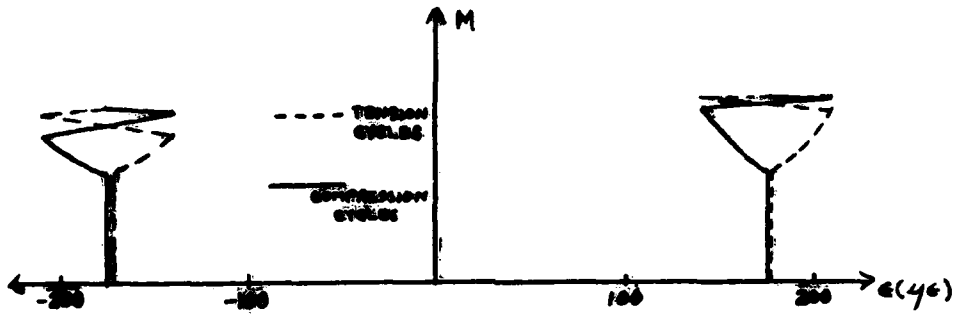

A mathematical basis for this process, using Equation (16), is offered below:

$$(16) \qquad \boxed{dM = \sum_i f_i \chi_\sigma(H_i)\,dH_i}$$

$$\Delta M_h = \chi_\sigma(H)h \qquad (f_i = 1 \text{ for applied field})$$

$$\Delta M_\sigma = (f+)\chi_\sigma(H)h - (f-)\chi_\sigma(0)h \qquad (\chi_\sigma \cong \chi_{rev} \text{ for field reversals})$$

$$\Delta M_{\bar{h}} = -\chi_\sigma(0)h$$

$$\Delta M_{\bar{\sigma}} = (f-)\chi_\sigma(0)h - (f+)\chi_\sigma(0)h$$

so, $\quad M_{h\bar{h}} = \chi_{(irr)}(H)h - \chi_\sigma(0)h = \chi_{(irr)}(H)h$

and $\quad M_{\sigma\bar{\sigma}} = \left[(f+)\chi_\sigma(H)h - (f-)\chi_\sigma(0)h\right] + \left[(f-)\chi_\sigma(0)h - (f+)\chi_\sigma(0)h\right]$

$\qquad = (f+)\chi_{irr}(H)h \qquad (\text{where } h_\sigma = h)$

taking the ratio of the two processes: $\dfrac{\Delta M_{\sigma\bar{\sigma}}}{\Delta M_{h\bar{h}}} = \dfrac{(f+)\chi_{irr}(H)h}{\chi_{irr}(H)h} = \underline{(f+)}$

The results of this experiment are shown graphically in Figure (14) for each of the applied fields used. It was observed that the populations (f+) and (f-) were equal within the ability to measure them. The readings taken at lower fields (<310 A/m) produced diffuse results since the induced magnet-

izations were near the detection limit. At higher fields, the results became very reproducable. The measurements showed an equality of (f+) and (f-) walls within two per-cent, independent of the applied field. This surprising result simplifies calculations considerably.

FIGURE 14

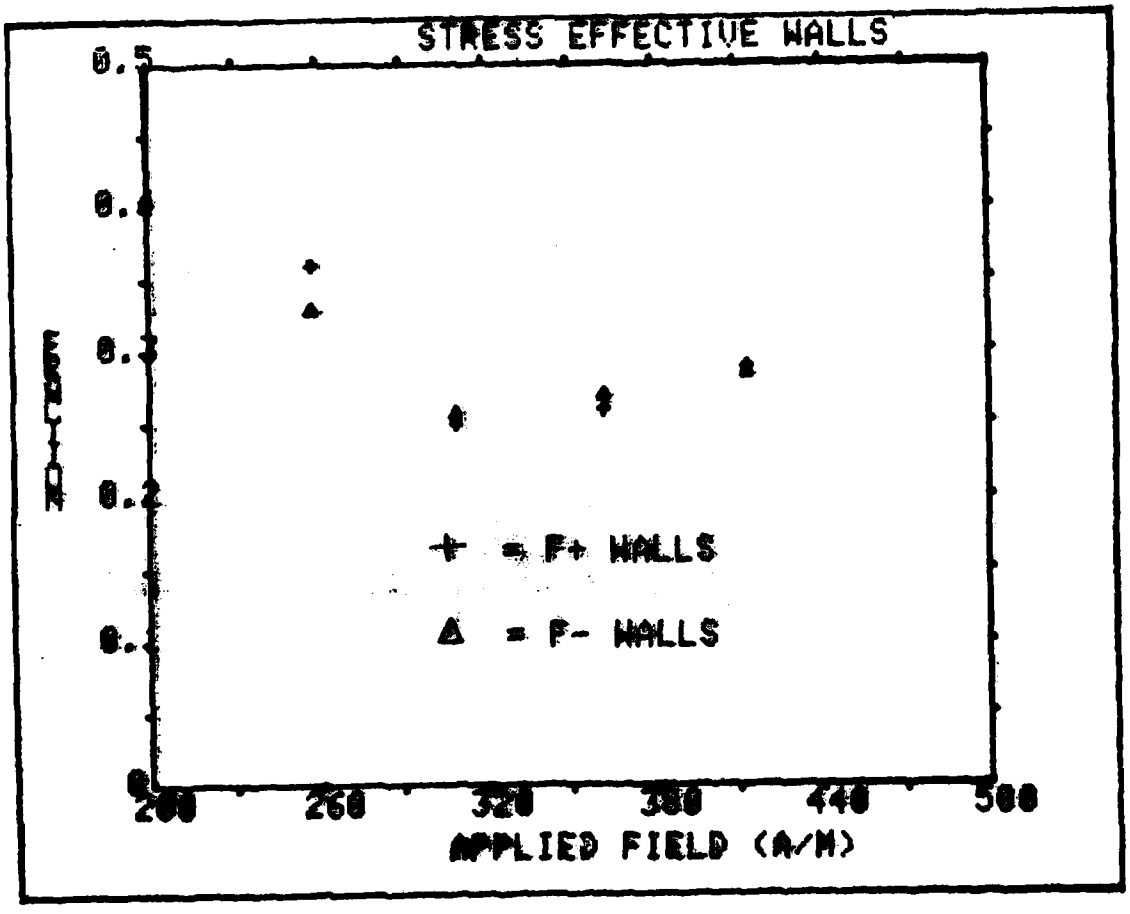

Figure (15) shows a comparison of the data taken in the compressive state and the tensile state. The comparison showed that the total stress-active population, (f+)+(f-), was greater in tension than in compression.

$$[(f+)+(f-)]_{tension} > [(f+)+(f-)]_{compression}$$

FIGURE 15

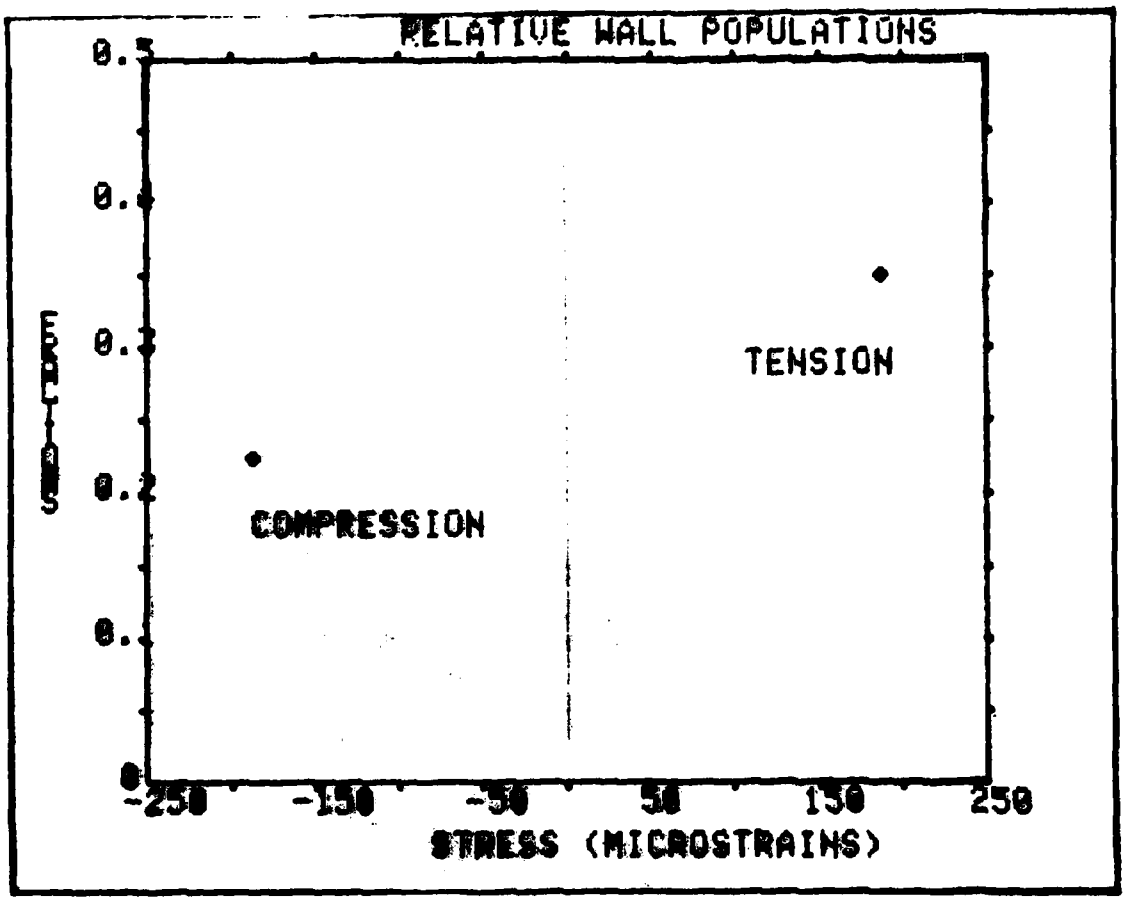

At the value of compression and tension used, 178 microstrains, the ratio of stress-active walls between tension and compression had reached a value of 1.56 ± .04. It is believed that the ratio is a function of stress, since the ratio must be unity in the case of zero applied stress. In order to make a reasonable assumption as to the nature of this function, further experimentation is required.

The inequality of stress-active walls between tension and compression would lead one to predict a greater increase of stress-induced magnetization in tension than in compression.

Now that an understanding has been gained about the three effects as they act separately, their simultaneous effects will be analyzed. A graph of stress-induced magnetization is given in Figure (16).

FIGURE 16

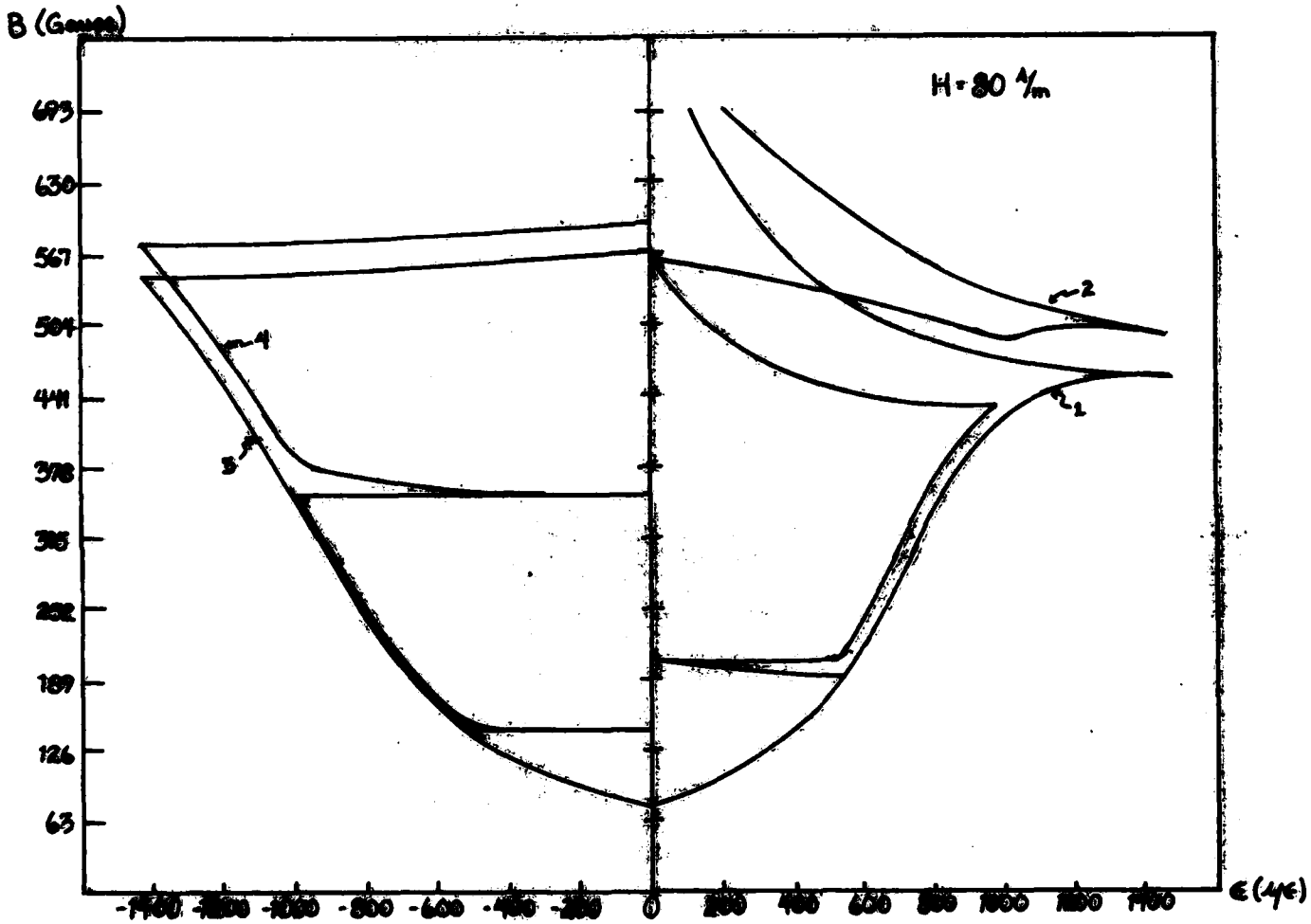

This figure is the cumulative display of four processes. Before stress was applied in each case, a field of 80 A/m was applied to magnetize the sample to point A. In the first process (curve 1), tension was applied continuously from zero to 1400 microstrains and back to zero. Curve 2 represents the application of tension again, however the

stress was cycled at 500 and 1000 microstrains. The third process was the continuous application of compression from zero to -1400 microstrains and back to zero. The fourth curve is the cycling of compression at -500 and -1000 microstrains. The sample was demagnetized between each of the four processes.

Certain characteristics of the graph have already been predicted from the effects already examined. There is a definite asymmetry in the application of tension and compression, with greater magnetization being seen in tension than for the equivalent value of compressive stress. This is due to the greater population of stress-active walls in tension. If the ratio of the slopes at +187 microstrains and -187 microstrains is taken, the value obtained is 1.61 ± .04, which agrees with the ratio of stress-active walls observed at that point, in the last section of data analysis. At higher values of stress, the simplicity seen in the lower stress values is destroyed due to multiple nonlinearities from other contributions.

It can be seen that for the stress-cycling, there is very little increase in the magnetization. This is especially notable in compression, where there is greater stability. This could be expected due to the equality of (f+) and (f-) walls. During the cycles, both walls are behaving according to Kondorsky's Law and are increasing the magnetization at the same rate, but in opposite directions. The sum of the equal but opposite effects is zero net magnetization.

There is some increase seen in tension for the first cycle. This is due to creeping, which is the gradual increase of magnetization due to cycling of stresses. The effect is more visible in tension than compression because of the greater population of stress active walls.

This inequality causes the magnetic behavior in tension to be 'amplified' in comparison to the compressive side of the graph. The change in the concavity of the magnetization curve is much more apparent in tension, and occurs at a lower value of stress than for compression. This is called the Villari reversal, which is due to the changing magnetostriction of iron. Iron will expand when a low magnetic field is applied to the material, but begins to contract in higher fields. This will result in a change of the sign of the magnetostriction constant, λ_s, and a subsequent reversal of the effects of stress on the material. This reversal is accounted for in the stress-effective field equation (Equation (5)) and in the stress-sensitive reluctance (Equation (9)), both of which depend on the magnetostriction constant.

Extremely nonlinear effects are seen in high tension. These arise from the simultaneous contributions of the three effects. At this stage, it is not possible to qualitatively evaluate these portions of the curve.

From the analysis up to this point, a very good understanding of the effects of stress on magnetization has been reached. The three separate effect of stress have

been identified and measured. The values derived from Equation (1) agree with the experimentally observed values, which indicates that this approach is fundamentally correct. The next step towards a complete understanding involves generating a magnetization curve from the relationships that have been evaluated in this research. This would require that a function for each of the three effects be programmed into a computer, and curves of the type seen in Figure (16) being produced from different inputs to this program. The inputs would include parameters such as the applied field, applied stress, and a "magnetic history" of the material.

REFERENCES

[1] R.R. Birss, C.A. Faunce, E.D. Isaac, "Magnetomechanical Effects in the Rayleigh Region," J. Phys. D. (Appl. Phys.), 14, 1971, p. 1040.

[2] W.F. Brown Jr., "Irreversible Magnetic Effects of Stress," Phys. Rev., 75, 1949, p. 149.

[3] C.S. Schneider and E.A. Semcken, "Vibration Induced Magnetization," J. Appl. Phys., 52, 1981, p. 1040.

[4] E.Kondorsky, J. Physics, (Moscow), 6, 1942.

[5] L.Lliboutry, "L'Aimantation des Aciers dans les Champs Magnetiques Faibles," Ann. Phys., (Paris), 6, 1951, p.731.

[6] L. Neel, Grenoble Univ., Ann. Math et Phys., 22, 1946, p.299.

[7] R.M. Bozorth, Ferromagnetism, D. Van Nostrand, New York, 1951, p.819.

APPENDIX A

DERIVATION OF IMPORTANT EQUATIONS

For the purposes of this paper, Equation (1) is the starting point of all derivations. Pairs of energy contributions are considered and the energy of the two terms is minimized. This method was suggested by R. M. Bozorth[7].

Equation (2): $\frac{\partial E_{H,K}}{\partial \theta} = -2k \sin\theta_{MK} \cos\theta_{MK} \cos 2\theta_{MK} + HM_s \mu_0 \sin\theta_{MH} = 0$

for polycrystalline material, the angular dependences are averaged isotropically (for solid angles):

so:

$$2k = HM_s \mu_0 (4)$$

or:

$$H_K = \frac{\pm 2k}{\mu_0 M_s (4)} = \boxed{\frac{\pm k}{2\mu_0 M_s}}$$

Equation (3) : $\frac{\partial E_{\sigma,K}}{\partial \theta} = -2k \sin\theta_{MK} \cos\theta_{MK} \cos 2\theta_{MK} + 3\lambda_s \sigma \cos\theta_{\sigma M} \sin\theta_{\sigma M} = 0$

again, after averaging for the solid angles:

$$\frac{3\lambda_s \sigma}{4} = \frac{2k}{8} \quad \text{or} \quad \boxed{\sigma_K = \frac{\pm k}{3\lambda_s}}$$

Equation (6): $\frac{\partial E_{M\sigma}}{\partial \theta} = -3\lambda_s \sigma \cos\theta_{MH} \sin\theta_{MH} + HM_s \mu_0 \cos\theta_{MH} = 0$

this follows from $\theta_{M\sigma} = (\theta_{MH} + 90)$ for transverse stress-field.

$\sin\theta_{M\sigma} = \sin(\theta_{MH} + 90) = \cos\theta_{MH}$ - then substitute into Equation (1) and differentiate to get the statement above.

$$HM_s \mu_0 = \pm \frac{3}{2} \lambda_s \sigma$$

$$H_\sigma (\text{transverse}) = \boxed{\pm \frac{3}{2} \frac{\lambda_s \sigma}{M_s \mu_0}}$$

Equation (4): The derivation is essentially the same as that for Equation (6), except that $\theta_{n\sigma} = \theta_{nu}$, which results in a sign reversal.

Equation (9): $\frac{\partial E_{nu}}{\partial \theta} = HM_s 4\pi \sin\theta_{nu} - \frac{DM_s^2 4\pi}{2} \sin\theta_{nu} = 0$

for our sample, $\theta_{nu} = -\theta_{nu}$, so after cancellation:

$$H_D = \frac{\pm DM_s}{2}$$

in the sample,

$$M = M_s \cos\theta_{nu} = \frac{\pm M_s}{2} \text{ after solid-angle averaging.}$$

$$\chi_D = \frac{M}{H_D} = \frac{1}{D} \quad \text{or} \quad \boxed{\chi_D^{-1} = D}$$

from Equation (6):

$$H_\sigma = \pm \frac{3}{2} \frac{\lambda_s \sigma}{M_s 4\pi} \quad \text{and from above: } M = \frac{\pm M_s}{2}$$

$$\chi_H = \frac{M}{H_\sigma} = \frac{M_s^2 4\pi}{3\lambda_s \sigma} \quad \text{or} \quad \boxed{\chi_H^{-1} = \frac{3\lambda_s \sigma}{M_s^2 4\pi}}$$

and for the total reluctance, χ^{-1}, one adds these two values with the inherent reluctance χ_{in}^{-1}, to get

$$\boxed{\chi^{-1} = \frac{1}{\chi_{in}} + D + \frac{3\lambda_s \sigma}{M_s^2 4\pi}}$$

All other equations are self-explanatory, or, in the case of Equation (16), it is proposed as a possible solution based upon the theoretical arguments presented in the text. This appendix should provide all proofs that are not obvious at first glance. They are set apart from the text in the hope of allowing smoother reading.

APPENDIX B-

SCHNEIDER'S RESTATEMENT OF KONDORSKY'S LAW IN TERMS OF THE DIFFERENTIAL SUSCEPTIBILITY

Kondorsky's Law in the Rayleigh region states:

$$M(H,\Delta H) = M(H) - 2M\left(\frac{\Delta H}{2}\right) \qquad (\Delta H < 2H)$$

where M is the magnetization of the material, H is an applied field, and ΔH is a small reversal of the field.

C. S. Schneider observed that since

$$\chi = \frac{dM}{dH} \qquad \text{or}$$

$$M = \int_0^H \chi \, dH$$

that the magnetization due to a field reversal could be expressed

$$M(\Delta H) = 2\int_0^{\Delta H} \chi(H')\,dH'$$

With a change of variables, this may be written:

$$M(\Delta H) = \int_0^{H} X\left(\frac{H}{2}\right) dH$$

This relation implies that

$$\chi_{\Delta}(\Delta H) = \chi\left(\frac{\Delta H}{2}\right) \qquad (\Delta H < 2H)$$

APPENDIX C-

ANALYSIS OF 3NiCr STEEL

Composition:

Fe- 94.25%
Ni- 2.94%
Cr- 1.62%
Mo- 0.48%
Mn- 0.30%
C - 0.14%
Al- 0.038%
S - 0.018%
P - 0.010%
Impurities- 0.204%

HY-80 Steel is austenitized at 1600 F for 72 minutes, water quenched, and tempered at 1290 F for 70 minutes.

Magnetic Constants:

Saturation Magnetization- 20,000 Gauss
Residual Magnetization from Saturation- 13,000 Gauss
Coercive Force- 650 A/m
Maximum Permeability- 910
Saturation Magnetostriction- 7.75 + .04 microstrains
Anisotropy Constant- 4300 J/m^3

APPENDIX D-

INDEX OF SYMBOLS USED

A- area enclosed by the B-coils on the cylindrical sample.

B- symbol for magnetization in the sample.

B-coil- coil of 100 turns on the sample which sensed the change in magnetization in the sample.

D- the demagnetizing constant resulting from the finite geometry of the sample.

E- Young's Modulus for the material.

(f+)- fractional population of (90+) walls.

(f-)- fractional population of (90-) walls.

(f_o)- fractional population of (180) walls.

(f_T)- total fractional population, normalized to unity.

H_a- applied external magnetic field.

H_{eff}- internal field seen by the material.

H_σ- stress-effective field.

k- anisotropy constant for the material

M- magnetization density in the sample

M_s- saturation magnetization density.

r- mean effective radius of the cylindrical sample.

R_B- resistance of the B-coil.

R_H- resistance of the H-coil.

V_B- voltage across the B-coil.

V_H- voltage across the H-coil.

ϵ- strain, a dimensionless quantity $\Delta l/l$ (fractional change in length).

μ_o- $4\pi \times 10^{-7}$ N/A^2

λ_s- saturation magnetostriction, the total fractional change in length when $M=M_s$.

χ- susceptibility (dM/dH).

χ_{m}- inherent susceptibility for the material.

χ_{rot} part of χ_{m} due to rotation inside the domains.

χ_{trans} part of χ_{m} due to translation of domain walls.

χ_{σ} - stress-sensitive susceptibility.

χ^{-1}- reluctance.

σ - stress

$\bar{\sigma}$ - removal of stress

UNCLASSIFIED

SECURITY CLASSIFICATION OF THIS PAGE (When Data Entered)

REPORT DOCUMENTATION PAGE

READ INSTRUCTIONS BEFORE COMPLETING FORM

1. REPORT NUMBER
U.S.N.A. - TSPR; no. 119 (1982)

2. GOVT ACCESSION NO.
AD-A124228

3. RECIPIENT'S CATALOG NUMBER

4. TITLE (and Subtitle)
THE EFFECTS OF TRANSVERSE STRESS ON MAGNETIZATION.

5. TYPE OF REPORT & PERIOD COVERED
Final.: 1981/1982

6. PERFORMING ORG. REPORT NUMBER

7. AUTHOR(s)
Richardson, John M.

8. CONTRACT OR GRANT NUMBER(s)

9. PERFORMING ORGANIZATION NAME AND ADDRESS
United States Naval Academy, Annapolis.

10. PROGRAM ELEMENT, PROJECT, TASK AREA & WORK UNIT NUMBERS

11. CONTROLLING OFFICE NAME AND ADDRESS
United States Naval Academy, Annapolis.

12. REPORT DATE
29 July 1982

13. NUMBER OF PAGES
45

14. MONITORING AGENCY NAME & ADDRESS(if different from Controlling Office)

15. SECURITY CLASS. (of this report)
UNCLASSIFIED

15a. DECLASSIFICATION/DOWNGRADING SCHEDULE

16. DISTRIBUTION STATEMENT (of this Report)
This document has been approved for public release; its distribution is UNLIMITED.

17. DISTRIBUTION STATEMENT (of the abstract entered in Block 20, if different from Report)
This document has been approved for public release; its dictribution is UNLIMITED.

18. SUPPLEMENTARY NOTES
Accepted by the U. S. Trident Scholar Committee.

19. KEY WORDS (Continue on reverse side if necessary and identify by block number)
Magnetization
Strains and stresses

20. ABSTRACT (Continue on reverse side if necessary and identify by block number)

The effects of transverse stress on the magnetization of 3NiCr steel were derived and observed in terms of three separate contributions. First, the previously determined stress-effective field was examined for transverse stress, and agreed with the results obtained in past experiments. A reversal of the effects of tension and compression was predicted and observed.

Second, the stress-sensitive reluctance was found to behave linearly

(OVER)

DD FORM 1 JAN 73 1473 EDITION OF 1 NOV 65 IS OBSOLETE
S/N 0102-LF-014-6601

UNCLASSIFIED

SECURITY CLASSIFICATION OF THIS PAGE (When Data Entered)

with tensile strain. The experimentally observed slope of 1.55±.05 correlated with the derived value of 1.60±.06. A lower limit to the reluctance was seen in compression.

The third effect was the fractional populations of stress-active domain walls. This is a newly postulated effect which accounts for large-scale changes in domain structure due to the application of external stress. The fractional populations of field-enhancing domain walls was observed to be equal to that od filed-reducing walls. Furthermore, the total population of stress-active walls was found to be a function of applied stress.